Waveguides and waveguide bends in two-dimensional photonic crystal slabs

Alongkarn Chutinan and Susumu Noda
Department of Electronic Science and Engineering, Kyoto University, Yoshida-honmachi, Sakyo-ku, Kyoto 606-8501, Japan
(Received 24 February 2000)

We present theoretical studies on waveguides and waveguide bends in two-dimensional photonic crystal slabs. The waveguides are created by either filling up or decreasing the sizes of air holes. Our designs focus on using the frequency range where the waveguide mode is nonleaky. It is shown that high transmission through the sharp bend can be obtained for some frequency ranges in the triangular lattice slabs. The waveguides in square lattice slabs are also investigated.

I. INTRODUCTION

Photonic crystals (PC) are optical materials with periodic changes in the dielectric constant, analogous to the crystal structure of a semiconductor, and band gaps can be created for certain ranges of photon energies.[1,2] Various applications are predicted and expected to be realized by photonic crystals, including ultrasmall optical circuits or optical integrated circuits (IC). Idealistically, such optical IC's should be realized by using the three-dimensional (3D) system,[3–5] but an alternative system using the dielectric slab with two-dimensional (2D) photonic crystal, or the 2D PC slab, also seems very attractive for its relatively easy fabrication.[6,7] It uses the effect of 2D PC to confine the light in the in-plane direction, and the refractive index contrast to confine the light in the vertical direction. Although the slab's guided modes can possess fairly large gaps and waveguides[8] or resonant cavities are shown to be possible,[9] the existence of leaky modes puts some constrains on designing waveguides in 2D PC slabs. To deal with leaky modes, one has two ways. One way is to examine the loss[10,11] and design the waveguides that give loss small enough to complete the signal processing. The other way is to avoid using leaky modes and use only nonleaky modes of the waveguides. In this work, we focus our designs on the latter, i.e., using nonleaky modes of the 2D PC waveguides. The structures studied in this work are (1) waveguides in the triangular lattice slabs for TE-like modes and (2) waveguides in the square lattice slabs for TM-like modes.

In Sec. II, we describe computational methods used in this work. We use the 3D finite-difference time-domain (FDTD) (Ref. 12) method with Bloch and Mur's[13] boundary conditions to calculate to band diagram of the PC. This method has been widely used for the band calculation of 2D PC slab.[14,15] The 3D FDTD with only Mur's boundary condition is used in simulation of the propagation of the light inside waveguides. In Sec. III, we describe the design for the waveguides in the triangular lattice slabs. The waveguides can be formed by filling up air holes with dielectric materials. Although this creates few waveguide modes, we use the frequency range that contains only a fundamental mode. In Sec. IV, the waveguides in the square lattice slabs are examined. Finally, the results are discussed and summarized in Secs. V and VI.

II. COMPUTATIONAL METHODS

We start with calculations of the band diagrams of 2D PC slabs and 2D PC slab waveguides by the 3D FDTD methods. For the calculation of band diagrams of 2D PC slabs, one period of the structure is mapped on the computational domain as shown in Fig. 1(a). The 2D PC slab is assumed to have periodicity in the *xy* plane. Therefore, the Bloch boundary condition, which is defined by

$$\mathbf{E}(\mathbf{r}+\mathbf{a},t)=\mathbf{E}(\mathbf{r},t)e^{i\mathbf{k}\cdot\mathbf{a}}, \quad \mathbf{H}(\mathbf{r}+\mathbf{a},t)=\mathbf{H}(\mathbf{r},t)e^{i\mathbf{k}\cdot\mathbf{a}},$$

where **a** is a primitive lattice vector and **k** is the wave vector, are applied at the four lateral edges parallel to the *z* axis. For the top and bottom edges perpendicular to the *z* axis, the

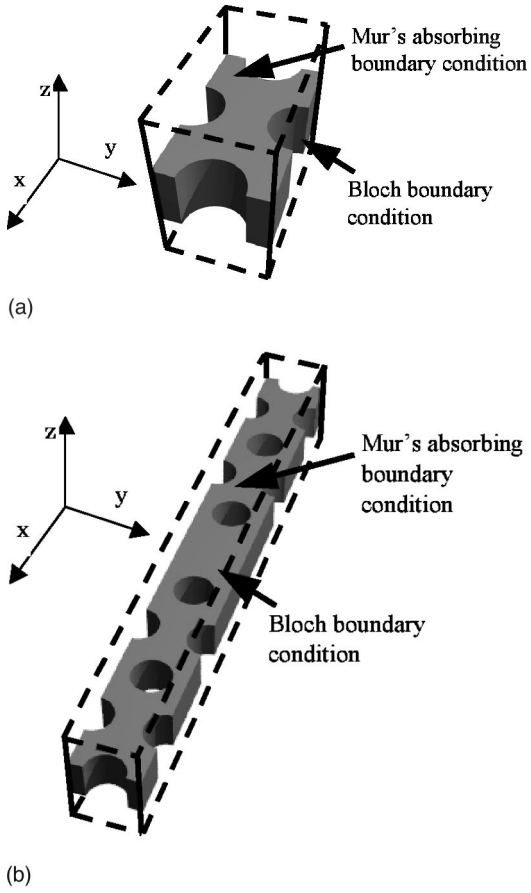

FIG. 1. Computational domains for the band calculations using the 3D FDTD method with Bloch and Mur's boundary condition. (a) One periodic cell for band calculations of the PC slabs. (b) The supercell for band calculations of the waveguides. The propagation direction of the waveguide is the *y* direction.

Mur's second-order absorbing boundary conditions are applied to absorb the waves leaked from the slab. First, broad Gaussian pulses are used to excite the electromagnetic (EM) eigenmodes of the slab over a wide range of frequencies. The EM fields at observation points are recorded for every time step and then Fourier transformed to obtain frequency spectra. The spectra will contain peaks at frequency values of the eigenmodes corresponding to the wave vector **k** given by the Bloch boundary condition. Second, we use narrow Gaussian pulses to excite every single eigenmode individually and to obtain the field pattern of such modes. We also perform a band calculation by the 2D plane-wave expansion (PW) method and obtain field patterns for every eigenmode. The effect of the finite thickness of the slab is approximated by using effective refractive index of the zeroth-order guided mode of the dielectric slab. Here, due to the fact that the field patterns of eigenmodes of 2D PC and 2D PC slab are almost identical, we can determine the correspondence of the eigenfrequencies and the band numbers exactly by comparing field patterns obtained by FDTD with those obtained by PW. For the calculation of the band diagram of 2D PC slab waveguides, we use a supercell with a waveguide as shown in Fig. 1(b). Infinite periods of the supercells are repeated spatially to form the waveguide in the y direction.

Next, we use 3D FDTD with Mur's boundary conditions at all six edges to calculate the propagation of EM waves inside the waveguides and the waveguide bends. We also calculate the propagation of EM waves inside the waveguides with bends in infinitely high 2D systems and compare the results with the 3D one.

III. WAVEGUIDE IN TRIANGULAR LATTICE SLAB

In this section, we study waveguides in triangular lattice slabs. Although the triangular lattice possesses a very large slab-mode gap for TE-like waves, the larger gap requires the larger filling factor of air holes and this leads to making all modes at the gap frequencies leaky and the structure more fragile. Therefore, we choose the filling factor of air holes to be ~ 0.3 or radii of air holes to be $0.29a$, where a is the lattice constant. The thickness of slab is chosen to be $0.6a$. The refractive index of the dielectric slab is assumed to be 3.4 corresponding to silicon at 1.55 μm throughout the paper. Air claddings are assumed at both sides of the slab to obtain strong confinement of the light inside the slab. We use the method described in Sec. II to calculate the band diagram of the PC slab for the TE-like mode. The result is shown in Fig. 2(a). The thick solid line shows the leaky mode region where every mode above this line is leaky. It is seen in Fig. 2(a) that a gap exists from frequency 0.256 to 0.320 [c/a]. Next, we create a waveguide by filling a row of air holes in the Γ-J direction. The band diagram of the waveguide is calculated and the result is shown in Fig. 2(b). In Fig. 2(b) the gray areas show the PC slab modes that can propagate inside the PC slab. The thick solid line shows the leaky mode region where every mode above this line is leaky as the same as in Fig. 2(a). The thin broken lines show leaky waveguide modes, and finally the thin solid lines show nonleaky waveguide modes. It is important that we use air claddings for both sides of the slab or the area of the leaky mode will become larger as shown by a thick broken line, where SiO_2

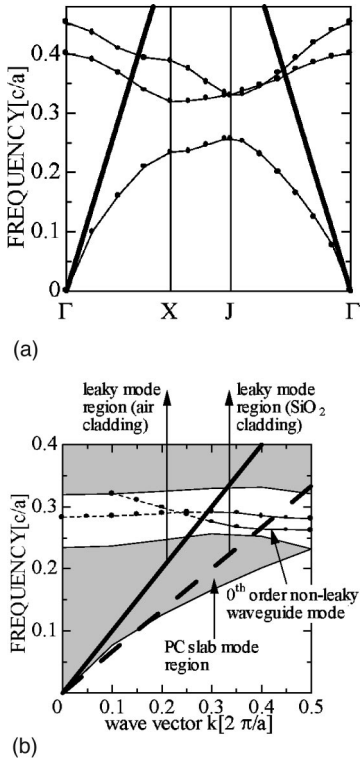

FIG. 2. Band diagrams for TE-like modes of (a) the triangular lattice slab and (b) the waveguide in the triangular lattice slab. The thick solid line shows the leaky mode region where every mode above this line is leaky for air cladding. The gray areas show the PC slab modes that can propagate inside the PC slab. The thick broken line shows the leaky mode region for SiO_2 cladding. The thin broken lines show leaky waveguide modes and the thin solid lines show nonleaky waveguide modes. The zeroth-order nonleaky waveguide mode (for air cladding) spans from frequency 0.27 to 0.28 [c/a], where there is no other waveguide mode.

cladding is utilized. In Fig. 2(b), the zeroth-order nonleaky waveguide mode (for air cladding) spans from frequency 0.27 to 0.28 [c/a], where there is no other waveguide mode. It is this frequency range where we practically achieve a nonleaky, single waveguide mode. We note that at the frequency range from 0.28 to 0.29 [c/a], there is a higher order mode that is nonleaky but there also exists a leaky mode at the same time so that the waveguide modes are not single.

Next step, we examine the properties of the waveguide with bends. A waveguide with two 60° bends like those shown in Fig. 3(a) is assumed for calculation. The distance between two bends is 16 layers. We simulate the propagation of light inside this waveguide by 3D FDTD. The Gaussian pulse is sent down the waveguide to calculate the transmission and reflection spectra.[16] Figure 3(b) shows the transmission and reflection spectra of the waveguide. It is seen that high transmissions of more than 90% can be obtained for a frequency range from 0.2703 to 0.2727 [c/a]. We can observe the field pattern of the waveguide mode by using CW excitation. Shown in Fig. 3(c) are amplitudes of z components (perpendicular to the surface of the paper) of the magnetic fields in the vicinity of the bend for the case where frequency is 0.2715 [c/a]. The dark and the bright spots correspond to the negative and positive values of the amplitude

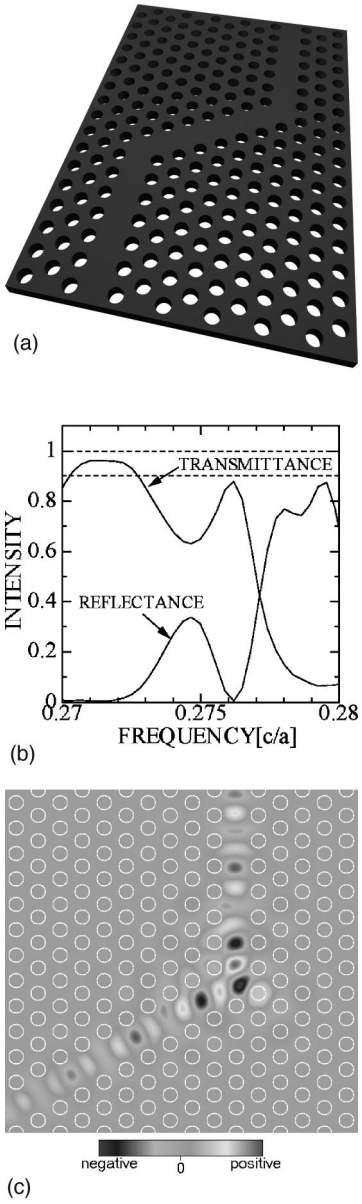

FIG. 3. (a) Schematic of the 2D PC slab waveguide with two 60° bends. (b) Transmission and reflection spectra of the waveguide with bends calculated by using 3D FDTD. (c) Z components of magnetic fields in the vicinity of the bend for frequency 0.2715 [c/a].

as indicated at the bottom of the figure. As discussed in Sec. II, the PC slab modes possess very similar field distributions to those of the modes of the infinitely high 2D PC, therefore, it is expected that the characteristics of the waveguides created in the PC slab and the 2D PC may resemble each other. For comparison, we create the waveguides with the same configuration as in Fig. 3(a) except it is infinitely high and use 2D FDTD to calculate the transmission and reflection spectra. The refractive index of 2.76 is used in the 2D calculation, as it is an effective refractive index for the zeroth-order TE wave confined in the dielectric slab. Figure 4(a) shows transmission and reflection spectra of the 2D case. It is seen that both results of 3D and 2D cases are similar, e.g., the transmittance drops largely near the frequency 0.278–0.28 [c/a]. This means that 2D calculations using an effective index give good approximations of the 3D calculations and

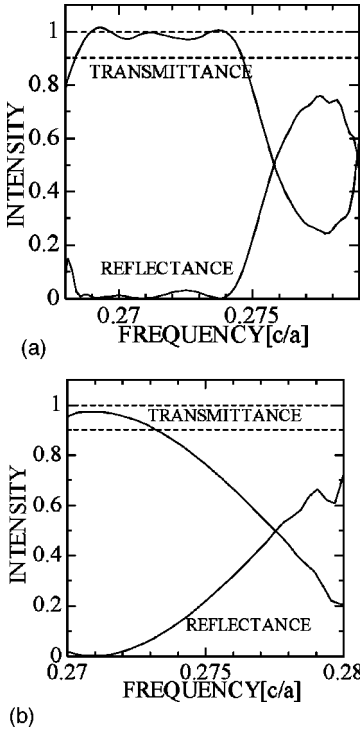

FIG. 4. Transmission and reflection spectra of (a) the infinitely high 2D PC waveguide with the same configuration as Fig. 3(a), and (b) the waveguide with only one 60° bend.

can be very useful in reducing computational resources and times. We note that a little change in an effective refractive index assumed will only shift the frequencies of the waveguide modes but the properties of the transmission and reflection spectra will remain the same as properties. In Fig. 4(b) we show transmission and reflection spectra of the waveguide with only one 60° bend calculated by using 2D FDTD with effective index. The transmittance is approximately 1 at lower frequencies and begins to decrease at higher frequencies. It is worth noting that, by comparing Fig. 4(b) with Figs. 3(b) and 4(a), we can see that peaks at frequency near 0.275 [c/a] originate from the resonance between two bends.

IV. WAVEGUIDE IN SQUARE LATTICE SLAB

In this section, we study waveguides for TM-like mode in the square lattice slab. For a 2D PC with a square lattice, a large TM mode band gap can be created with dielectric rods in air background. Using air rods in dielectric backgrounds also provide a large TM mode band gap but this again requires a large filling factor of air rods which is unfavorable as discussed in Sec. II. Also we have seen in Sec. II that although we can choose a filling factor that creates a large gap, the existence of higher order waveguide modes limits the range of frequencies that contains only a single waveguide mode. Therefore, we choose the filling factor of air holes to be $\sim$0.6 or radii of air holes to be 0.437a and the thickness of the slab to be 2.5a to provide a TM-like mode gap of 5–7% in width. It is found that thinner slabs provide smaller gaps and the thickness less than 1.0a does not create a gap. This difference of our slab thickness for TE-like and TM-like mode agrees well with the previous analysis on the

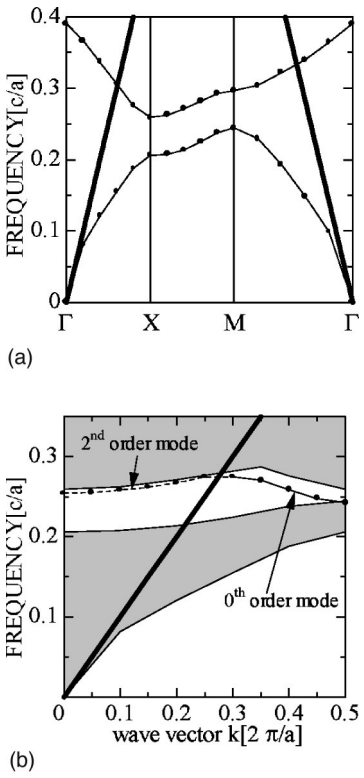

FIG. 5. Band diagram for the TM-like mode of (a) the square lattice slab and (b) the waveguide in the square lattice slab. The zeroth-order nonleaky mode spans from frequency 0.248 to 0.254 [c/a].

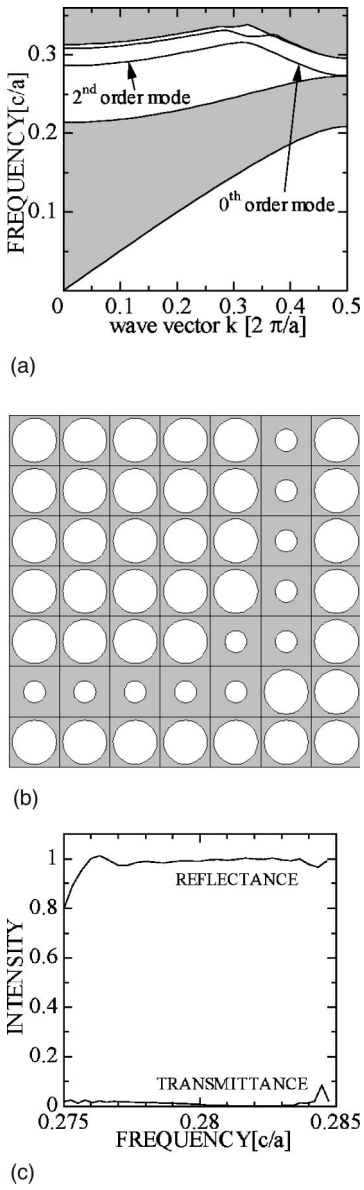

FIG. 6. (a) Band diagram for the TM mode of the infinitely high square lattice. The zeroth-order mode spans from frequency 0.275 to 0.285 [c/a]. (b) Schematic of the 90° bend in the square lattice. (c) Transmission and reflection spectra of the bend computed by 2D FDTD.

PC slab mode, though for TM-like mode, dielectric rods were assumed in Ref. 7 where we assume air rods. Figure 5(a) shows a band diagram of the square lattice slab. There is a gap from 0.244 to 0.259 [c/a]. Next, to create a waveguide, one can fill up a row of air holes but the frequencies of the waveguide mode created will lie low outside the band gap which means it will leak outside to the PC area. The fold back of this waveguide mode that lies inside the gap also lies inside the leaky mode region. Therefore, we create a waveguide by changing radii of a row of air holes to be $0.38a$. This gives a band diagram as shown in Fig. 5(b). We can see in Fig. 5(b) that there is a second-order mode and a fold back of zeroth-order mode. It is this zeroth-order mode that we are looking for near wave vector $\mathbf{k}=0.5[2\pi/a]$. At smaller k near $k=0.35[2\pi/a]$, the zeroth-order mode begins to mix up with the second-order mode and becomes more complicated. After all, the frequency range where there exists only a zeroth-order mode and no other mode is from 0.248 to 0.254 [c/a].

We tried to calculate the transmission spectrum of the waveguide with 90° bend by using 3D calculation but the gap is so small that it needs a far larger computational domain than that in Sec. III. Nevertheless, we can examine the properties of this waveguide bends through the infinitely high 2D PC as discussed in Sec. III. Figure 6(a) shows a band diagram of 2D PC assumed in the calculation. The filling factor is the same as the above and refractive index assumed is 2.82. There is a zeroth-order mode spanning from frequency 0.275–0.285 [c/a]. First, we confirm by 2D FDTD calculation that the EM waves can propagate along the straight waveguides without loss. We then calculate the transmission and reflection spectra of the waveguide bend. The configuration of the bend is shown in Fig. 6(b) and the spectra are shown in Fig. 6(c). It is seen that almost all waves are reflected from the bend. This result will be discussed in the next section.

V. DISCUSSIONS

We have investigated the waveguides in 2D PC slabs in both triangular lattices and square lattices. They are created by either filling up or decreasing the sizes of air holes, i.e., dielectric materials are added into the PC to create the waveguide modes. We shall refer to this as ''dielectric waveguides.'' This is in contrast with PC waveguides previously reported where dielectric materials are removed, i.e.,

some dielectric materials are replaced by air.[5,17] This shall be referred to as ''air waveguides.'' Removing a small amount of dielectric material will lift up one dielectric band (the band lower than the band gap) into the frequency range of the band gap and create a waveguide mode confined in the air. Adding a small amount of dielectric material will pull down few air bands (the band higher than the band gap) and create few waveguide modes confined in the dielectric. Some of these waveguide modes are the higher-order modes, and some are actually the fold backs of the lower-order modes. In this study, we have focused on using nonleaky parts of the fold backs of the zeroth-order waveguide modes created. The calculations show that high transmission (>90%) through the sharp bend can be obtained for some frequency ranges in the triangular lattice slabs for TE-like waves. But for TM-like waves in square lattice slabs, almost all frequencies are reflected from the bend.

The characteristics of the waveguide bends in both lattices considered here are seen different from those in infinitely high 2D PC's (Ref. 17) and 3D PC's (Ref. 5) where high transmission can be obtained over a wide range of frequencies. The fundamental difference in their structures and modes of the waveguides may provide an explanation for this. In Ref. 17, Mekis *et al.* modeled the transmission of waves through the bends in the square lattice 2D PC as a scattering process in which the mode propagating along the (01) direction is scattered into the transient mode propagating along the (11) direction, then into the mode propagating along the (10) direction. For the case of air waveguides, there is only one transient mode at the bend. But for the case of dielectric waveguides, there is more than one transient mode so that the mode coupling can be more complicated. Therefore, it seems likely that the characteristics of high transmission over a wide range of frequencies are observed in air waveguides rather than in dielectric waveguides. In fact, beside the high transmission for TM waves in 2D PC's using air waveguides,[17] we have calculated the transmission for TE waves in the square lattice 2D PC's using air waveguides and found the similar characteristic while we could not find it in the cases of dielectric waveguides examined in this paper.

Finally, we suggest that uninvestigated designs for the 2D PC slab waveguides using air-confined waveguide modes should also be investigated. These modes can be achieved by either enlarging the size of air holes or replacing some parts of dielectric with low-index material. Although it may seem that waveguide modes of this kind should be very leaky in the 2D PC slab, we expect that by choosing appropriate parameters they can be nonleaky for ranges of frequencies not smaller than those of the dielectric modes discussed in this paper.

VI. SUMMARIES

In this paper, we have presented the designs for waveguides in 2D PC slabs for both TE-like and TM-like modes in triangular lattices and square lattices, respectively. The waveguides are created by either filling up or decreasing the sizes of air holes. We have focused on using nonleaky parts of the fold backs of the zeroth-order waveguide modes created. It is shown that high transmission (>90%) through the sharp bend can be obtained for some frequency ranges in the triangular lattice slabs for TE-like waves. But for TM-like waves in square lattice slabs, almost all frequencies are reflected from the bend.

ACKNOWLEDGMENT

This work was partly supported by a grant-in-aid for scientific research of priority areas from the Ministry of Education, Science and Culture of Japan.

[1] E. Yablonovitch, Phys. Rev. Lett. **58**, 2059 (1987).
[2] S. John, Phys. Rev. Lett. **58**, 2486 (1987).
[3] S. Noda, N. Yamamoto, and A. Sasaki, Jpn. J. Appl. Phys., Part 2 **35**, L909 (1996).
[4] S. Noda, N. Yamamoto, M. Imada, H. Kobayashi, and M. Okano, J. Lightwave Technol. **17**, 1948 (1999).
[5] A. Chutinan and S. Noda, Appl. Phys. Lett. **75**, 3739 (1999).
[6] T. F. Krauss, R. M. De La Rue, and S. Brand, Nature (London) **383**, 699 (1996).
[7] T. Baba, N. Fukaya, and J. Yonekura, Electron. Lett. **35**, 654 (1999).
[8] S. G. Johnson, S. Fan, P. R. Villeneuve, and J. D. Joannopoulos, Phys. Rev. B **60**, 5751 (1999).
[9] O. J. Painter, A. Husain, A. Scherer, J. D. O'Brien, I. Kim, and P. D. Dapkus, J. Lightwave Technol. **17**, 2082 (1999).
[10] I. El-Kady, M. M. Sigalas, R. Biswas, and K. M. Ho, J. Lightwave Technol. **17**, 2042 (1999).
[11] H. Benisty, D. Labilloy, C. Weisbuch, C. J. M. Smith, T. F. Krauss, D. Cassagne, A. Béraud, and C. Jouanin, Appl. Phys. Lett. **76**, 532 (2000).
[12] K. S. Yee, IEEE Trans. Antennas Propag. **AP-14**, 302 (1966).
[13] G. Mur, IEEE Trans. Electromagn. Compat. **EMC-23**, 377 (1981).
[14] M. Boroditsky, R. Coccioli, and E. Yablonovitch, Proc. SPIE **3283**, 184 (1998).
[15] O. J. Painter, J. Vuckovic, and A. Scherer, J. Opt. Soc. Am. B **16**, 275 (1999).
[16] Because the frequency range of the waveguide mode is very narrow, the pulse spans over more than 100 periods of PC and this requires hundreds of periods of PC regions in 3D. We used a parallelized version of 3D FDTD to achieve this.
[17] A. Mekis, J. C. Chen, S. Fan, P. R. Villeneuve, and J. D. Joannopoulos, Phys. Rev. Lett. **77**, 3787 (1996).